Proposal of Double-Sided Transverse Flux Linear Synchronous Motor and a Simplified Design for Maximum Thrust in Nonsaturation Region

Jung-Seob Shin[1], Takafumi Koseki[1], and Houng-Joong Kim[2]

[1]Department of Electrical Engineering, Graduate School of Engineering, The University of Tokyo, Bunkyo-ku, Tokyo 113-8656, Japan

[2]KOVERY Co. Ltd., Gosaek-dong, Gwonseon-ku, Suwon, Gyeonggi-do 441-813, Korea

We propose a double-sided, transverse flux linear synchronous motor to address the problem of the complex structure of transverse-flux machinery. A design method for maximum thrust in a nonsaturation region is then proposed as a simplified approach. Finally, the usefulness of the proposed method are analyzed and evaluated by using a 3-D finite element method.

***Index Terms*—Equivalent reluctance network method, linear synchronous motor, thrust design, transverse flux type machinery.**

I. Introduction

LARGE THRUST is one of the performance requirements for the permanent magnet linear synchronous motor (PMLSM). The transverse-flux machinery (TFM) is suitable for a large-thrust design [1]. However, the manufacturing process for conventional TFMs is difficult because of the complex structure resulting from the 3-D magnetic circuit [2], [3]. In the conventional manufacturing process, a large number of segmented components are needed to make up the magnetic circuit, and the use of lamination is difficult.

The estimation of the design point at which maximum thrust is obtained is important in the preliminary design stage because it saves design time. In a previous study, we proposed a theoretical design of thrust for a simple estimation [4]. It proved useful for finding the maximum thrust under a condition in which only the structure and total volume are known. However, the method is not effective when magnetic saturation occurs because of the linear characteristic between the thrust and current. If the design point from the previous study is positioned in the saturation region where there is a nonlinear characteristic between thrust and current, losses increase and control performance deteriorates, which degrades motor performance [5], [6]. Therefore, it is important to estimate the flux related to magnetic saturation and its position and develop a design for maximizing thrust in the range where magnetic saturation does not occur.

In this paper, we propose a double-sided transverse flux linear synchronous motor to address the problem of the complex structure in TFM and a simplified design method for maximum thrust in nonsaturation region in the preliminary design stage. In Section II, operational principle and structural advantages are introduced. In Section III, a simplified design for maximum thrust in a nonsaturation region is described. Finally, in Section IV, the usefulness of the proposed method is analyzed and evaluated by 3-D finite element method (FEM).

Manuscript received November 04, 2012; revised December 18, 2012, December 24, 2012; accepted December 27, 2012. Date of current version July 15, 2013. Corresponding author: J.-S. Shin (e-mail: jungseobshin1008@koseki.t.u-tokyo.ac.jp).

Color versions of one or more of the figures in this paper are available online at http://ieeexplore.ieee.org.

Digital Object Identifier 10.1109/TMAG.2013.2237761

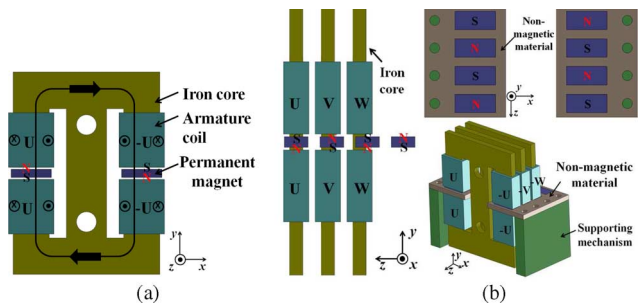

Fig. 1. The basic configuration of the three-phase unit. (a) Armature and field units. (b) Configuration along the moving direction. (In (a), black arrows denote flux flow under a no-load condition. In (b), −U, −V, and −W are present components shifted by 180 degrees from U, V, and W).

II. Operational Principle and Structural Advantages

Fig. 1 shows the basic configuration of the three-phase unit of the proposed model. The armature unit—which is the mover—consists of an iron core and four coils; the field unit—which is the stator—consists of two magnets. The two coils on the left side are wound in a direction opposite to those on the right side, and these coils are connected in series, as shown in Fig. 1(a). Armature cores and magnets are arranged along the moving direction z, as shown in Fig. 1(b). Each core is spatially separated by 120 degrees difference. Field magnets are fixed in a nonmagnetic material plate and each magnet is electrically separated by 180 degrees. By applying AC current with 120-degree phase difference to armature coil, the proposed model operates as a 3-phase AC synchronous motor.

Unlike the configuration in conventional TFM, the proposed model has a 2D magnetic circuit in which the main flux from the north pole flows transversely to the south pole along an armature core, as shown in Fig. 1(a). This magnetic circuit eases manufacturing because of the following reasons:

a) Simple structure: Only two magnets and one armature core, which is not segmented, are required to construct the magnetic circuit.
b) Use of lamination: The iron core is easily fabricated using laminated steel plates.
c) Small sensitivity of normal attractive force to assembly error: It has been reported that normal attractive force reaches the same level as that of thrust with an air gap

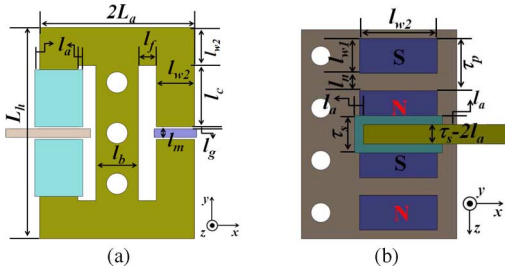

Fig. 2. Specifications of parts. (a) x-y plane. (b) x-z plane. (In (a), armature coils and nonmagnetic material on the right side are removed for clarity).

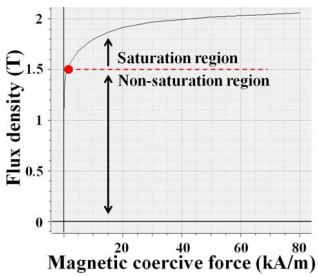

Fig. 3. B-H characteristic of 50JN230.

TABLE I
DESIGN SPECIFICATIONS AND MATERIALS [8], [9]

Symbol	Quantity	Symbol	Quantity	Symbol	Quantity
L_a [mm]	40	l_f [mm]	10	l_g [mm]	1
L_h [mm]	100	l_b [mm]	20	l_n [mm]	2
$_p$ [mm]	13.5	l_{w1} [mm]	11.5	l_a, l_m	Variables
$_s$ [mm]	9	l_{w2} [mm]	20	l_c [mm]	

Materials	Note	Materials	Note
50JN230	Iron core	N50M	Magnet (NdFeB,Br:1.4T)

imbalance of only 0.5 mm, resulting from the use of two independent magnetic circuits in a conventional double-sided configuration [7]. However, in the proposed model, the magnetic circuit is not independent and mainly changes irrespective of whether there is an air gap imbalance because the total magnetic air gap is constant. Thus, the burden placed on the supporting mechanism is small, and manufacture is easy.

III. THE SIMPLIFIED DESIGN FOR MAXIMUM THRUST IN NONSATURATION REGION

A. Specification and Materials in the Proposed Design

Figs. 2 and 3, and Table I show specifications of parts and materials used in the proposed model.

We focused on the thrust in a one-phase configuration because thrust in a three-phase configuration can be estimated from the results obtained in the one-phase configuration. All dimensions, except for l_a, l_c, and l_m, are fixed and are selected on the basis of spatial limitations. A total volume of 80 mm × 100 mm × 27 mm and three-core/two-pole combination were selected. In this volume, the pole pitch, τ_p, and slot pitch, τ_s, are 13.5 and 9 mm, respectively. In Fig. 3, 1.5 T denotes the maximum flux density in the nonsaturation region [8].

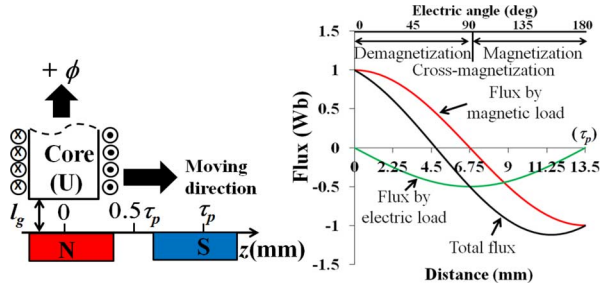

Fig. 4. Flux distribution in the armature core due to armature reaction. (The positive value on the left side represents the direction in which the flux flows into the iron core).

B. Key Design Variables in the Proposed Design

Key design variables are l_a, l_c, and l_m. Variables l_a and l_c denote the half slot length in the moving direction and the height in the space in which the armature coil is wound, respectively. They are related to the electric load, NI, which represents the magnetomotive force (MMF) on the armature side. It depends on the space in the total volume and is expressed as (1). In (1), $N(l_a, l_c)$ is the number of windings per armature pole; I is armature current; α is packing factor of coil; $A_w(l_a, l_c)$ is the cross-section area where the armature coil is wound; S_c is dimension of the armature coil; and J is current density. From (1), $N(l_a, l_c)$ is proportional to l_a and l_c.

$$N(l_a, l_c)I = \frac{\alpha A_w(l_a, l_c)I}{S_c} = \alpha A_w(l_a, l_c)J(A_w(l_a, l_c) = l_a \times l_c) \quad (1)$$

The term l_a affects the width, l_z, and cross-section, A_a, of the armature core, as expressed in (2). $A_a(l_a)$ is inversely proportional to $N(l_a, l_c)$ under the same τ_s

$$A_a(l_a) = l_z(l_a) \times l_{w2} \quad (l_z(l_a) = \tau_s - 2l_a). \quad (2)$$

The variable l_m is the magnet length in the magnetization direction. It is related to the magnetic load that represents the MMF of the field magnet, depends on the space of the total volume, and is expressed as $H_c l_m$. The relation between l_m and l_c is given in (3). From (1) and (3), $N(l_a, l_c)$ is inversely proportional to $H_c l_m$ under the same l_a

$$l_m = L_h - 2(l_g + l_c + l_{w2}). \quad (3)$$

C. Simple Estimation of Maximum Flux in the Armature Core by Armature Reaction and Its Position

Whether the design point is in nonsaturation region or not depends on the maximum flux in the armature core, and the amount of the flux depends on magnetic and electric loads. When sinusoidal current is applied to the armature coil under a condition in which the d-axis current is maintained at zero, flux distribution in the armature core due to armature reaction is as illustrated in Fig. 4.

When z is equal to 0, the total flux is equal to the flux generated by the magnetic load because the armature current is equal to zero. When the armature core is between zero and 0.5 τ_p, the total flux decreases because of demagnetization. When z is

equal to 0.5 τ_p, the total flux in the iron core is equal to the flux generated by the electric load. This is because of cross-magnetization. When the armature core is between 0.5 τ_p and τ_p, the total flux increases because of magnetization. If magnetic saturation is negligible, nonlinear characteristics in saturation region is also negligible. Therefore, the total flux is calculated by the principle of superposition, as expressed in (4). In (4), $\phi_{\rm tl}$, $\phi_{\rm ml}$, and $\phi_{\rm el}$ denote total flux and the flux generated by the magnetic and electric loads. Also, $\phi_{\rm ml\_max}$ and $\phi_{\rm el\_max}$ denote the maximum values generated by both loads at $z = 0$ and 0.5 τ_p, where both loads affect $\phi_{\rm tl}$ independently

$$\begin{aligned}\phi_{\rm tl}(z) &= \phi_{\rm ml}(z) - \phi_{\rm el}(z) \\ &= \phi_{\rm ml\_max}\cos\left(\frac{\pi z}{\tau_p}\right) - \phi_{\rm el\_max}\sin\left(\frac{\pi z}{\tau_p}\right). \quad (4)\end{aligned}$$

Only one maximum point exists between 0 and τ_p. The position of the point $z_{\rm \_max}$ is obtained, expressed as (5). The flux density in the armature core in this position, $B_{\rm max}$, is calculated by (6). One necessary condition to avoid magnetic saturation is that $B_{\rm max}$ must be lower than 1.5 T

$$\frac{d\phi_{\rm tl}(z)}{dz} = 0 \rightarrow z_{\rm \_max} = \frac{\tau_p}{\pi}\tan^{-1}(-A) + \tau_p \left(A = \frac{\phi_{\rm el\_max}}{\phi_{\rm ml\_max}}\right) \quad (5)$$

$$B_{\rm max} = \frac{\phi_{\rm tl}(z_{\rm max})}{A_a(l_a).} \quad (6)$$

The term $z_{\rm \_max}$ depends on the ratio of the flux generated by electric and magnetic loads, A, as shown in Fig. 5. The position of the maximum point approaches from τ_p to 0.5 τ_p with increase in A. The total flux at $z_{\rm \_max}$ is greater than $\phi_{\rm ml\_max}$, in all the range of A. Another necessary condition to avoid magnetic saturation is that the flux density in the armature core at $z = 0$ must be lower than 1.5 T. The behavior in V and W phases is the same as that in the U phase, except for $z_{\rm \_max}$.

If $B_{\rm max}$ is larger than 1.5 T at certain design point, it means that the design point is in the saturation region. Hence, there exist differences between theoretical values based on the principle of superposition and real values due to nonlinear characteristics in saturation region. However, an exact value in saturation region is not important in the proposed design because $B_{\rm max}$ are only used to confirm whether the design point is in saturation region or not.

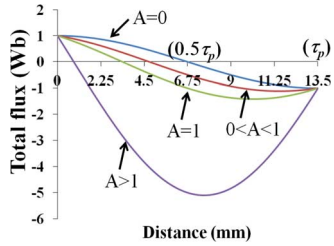

Fig. 5. Total flux distribution by the flux ratio A.

D. Calculation of $\phi_{\rm ml\_max}$ and $\phi_{\rm el\_max}$

The equivalent reluctance network (ERN) method has been employed for the calculation of $\phi_{\rm ml\_max}$ and $\phi_{\rm el\_max}$ because it offers the advantage of a very short computation time [6], [10]. Fig. 6 shows magnetic circuit models. We have employed a 2-D ERN method to facilitate simple calculation. The models and each reluctance component used in our calculation are linear and have been determined on the basis of [6], [10]. In Fig. 6, z is the width of each area; R_g is the magnetic reluctance in the air; and H_m is the magnetic-field component of the magnet at the operating point. The components related to $\phi_{\rm el\_max}$ and $\phi_{\rm ml\_max}$ are $\phi_{\rm el\_I}$ and $\phi_{\rm ml\_III}$, respectively. They are calculated from (7) to (13), where $\phi_{\rm \_j}$, R_{g_j}, and $M_{\rm \_j}$ are flux, magnetic reluctance, and MMF matrices, respectively, see (7)–(13) at the bottom of the page.

E. Process of Thrust Calculation

Because thrust depends on electric and magnetic loads and these loads are determined by l_a and l_m, we have focused on l_a and l_m. Below is the process of thrust calculation:

$$\phi_{\rm \_j} = R_{g\_j}^{-1} \times M_{\rm \_j} \quad (j = el, ml) \quad (7)$$

$$\phi_{\rm \_el} = [\phi_{el\_I}, \phi_{el\_II}, \phi_{el\_III}, \phi_{el\_IV}, \phi_{el\_V}]^T \quad (8)$$

$$\phi_{\rm \_ml} = [\phi_{\rm ml\_I}, \phi_{\rm ml\_II}, \phi_{\rm ml\_III}]^T \quad (9)$$

$$R_{g\_\rm el} = \begin{bmatrix} 2R_{g\_\rm el1} & -2R_{g\_\rm el1} & 0 & 0 & 0 \\ -2R_{g\_\rm el1} & 2R_{g\_\rm el2}+2R_{g\_\rm el3} & -2R_{g\_\rm el2} & 0 & 0 \\ 0 & -2R_{g\_\rm el2} & 2R_{g\_\rm el2}+2R_{g\_\rm el3} & -2R_{g\_\rm el3} & 0 \\ 0 & 0 & -2R_{g\_\rm el3} & 2R_{g\_\rm el3}+2R_{g\_\rm el4} & -2R_{g\_\rm el4} \\ 0 & 0 & 0 & -2R_{g\_\rm el4} & 2R_{g\_\rm el4}+2R_{g\_\rm el5} \end{bmatrix} \quad (10)$$

$$R_{g\_\rm ml} = \begin{bmatrix} 2R_{g\_\rm ml1}+2R_{g\_\rm ml2} & -2R_{g\_\rm ml2} & 0 \\ -2R_{g\_\rm ml2} & 2R_{g\_\rm ml2}+2R_{g\_\rm ml3} & -2R_{g\_\rm ml3} \\ 0 & -2R_{g\_\rm ml3} & 2R_{g\_\rm ml3} \end{bmatrix} \quad (11)$$

$$M_{\rm \_el} = [2N(l_a, l_c)I - H_m l_m, 0, H_m l_m, H_m l_m, 0]^T \quad (12)$$

$$M_{\rm \_ml} = [0, 0, H_m l_m]^T. \quad (13)$$

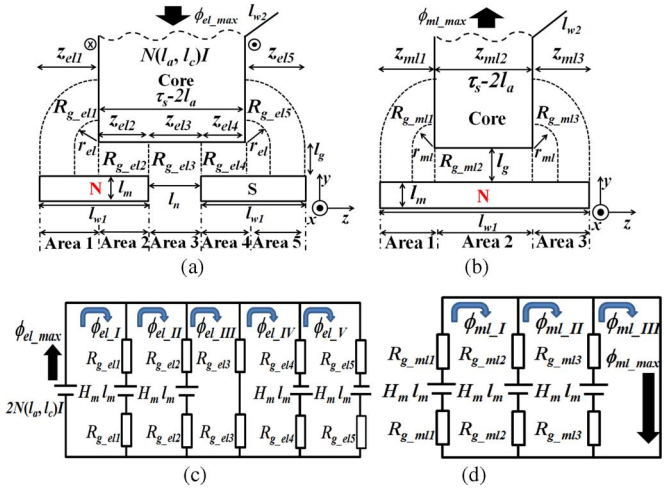

Fig. 6. Magnetic circuit models for flux calculation by electric and magnetic loads. (a) Model at $z = 0.5\ \tau_p$. (b) Model at $z = 0$. (c) Equivalent magnetic circuit at $z = 0.5\ \tau_p$. (d) Equivalent magnetic circuit at $z = 0$. (Only a half model is illustrated because of the symmetric structure).

TABLE II
SPECIFICATIONS IN ANALYSIS

Symbol	Quantity	Symbol	Quantity	Symbol	Quantity
J [A/mm^2]	7		0.7	l_a [mm]	1 ~ 3
I [A]	4.5	v [m/s]	1	l_m [mm]	4

a) determine constrains on l_a and l_m;
b) calculate $\phi_{\mathrm{el\_max}}$, and $\phi_{\mathrm{ml\_max}}$ at $z = 0, 0.5\tau_p$ from (7);
c) calculate $z_{\mathrm{\_max}}$ from (5);
d) calculate $\phi_{\mathrm{tl}}(z_{\mathrm{\_max}})$ and $B_{\max}$ from (4) and (6);
e) find the design point at which $B_{\max}$ is less than 1.5T;
f) calculate the thrust per phase $F_{t\_\max}$ in the design point.

The selected design point in (e) is the optimal design point, and $F_{t\_\max}$ is the maximum thrust in nonsaturation region. It is expressed as (14) by substituting $\phi_{\mathrm{ml\_max}}$ for flux in the armature core under a no-load condition as shown in [4]

$$F_{t\_\max} = p\frac{E_{\mathrm{rms}}I}{v} = \frac{\sqrt{2}p\pi\phi_{\mathrm{ml\_max}}N(l_a, l_c)I}{2\tau_p}. \qquad (14)$$

IV. ANALYSIS AND EVALUATION USING 3D FEM

Table II and Fig. 7 show the specifications in analysis and results from both theoretical and 3-D FEM analyses. The JMAG-Designer 10.4.3h commercial package was used for the 3-D FEM analysis [11], whose feasibility has been experimentally proven in [12]. There is a good agreement between theoretical values based on the 2-D ERN method and 3-D FEM values.

The amount by which $\phi_{\mathrm{ml\_max}}$ decreased and that by which $\phi_{\mathrm{el\_max}}$ increased with increase in l_a, resulting from decrease in the cross-section of the armature core and increase in electric load are shown in Fig. 7(a). Hence, the ratio of the flux generated by electric and magnetic loads, A, increased, as shown in Fig. 7(b). However, A was lower than 1 in all cases of l_a, which means that the total flux in this condition was affected by $\phi_{\mathrm{ml\_max}}$ rather than by $\phi_{\mathrm{el\_max}}$. Hence, total flux decreased when l_a increased, as shown in Fig. 7(c). On the other hand,

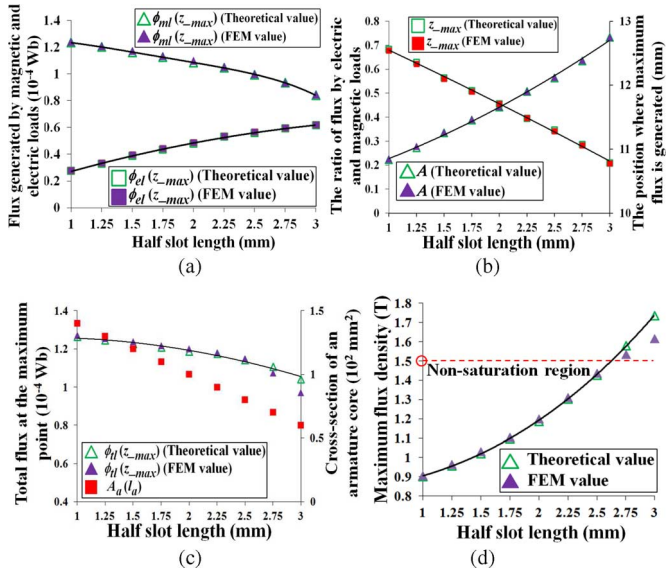

Fig. 7. Theoretical and 3-D FEM results. (a) $\phi_{\mathrm{ml\_max}}$ and $\phi_{\mathrm{el\_max}}$. (b) A and $z_{\mathrm{\_max}}$. (c) $\phi_{\mathrm{tl}}(z_{\mathrm{\_max}})$ and $\mathrm{A}_a(l_a)$. (d) $B_{\max}$.

TABLE III
RESULTS OF THRUST AT THE OPTIMAL POINT

F_{t_max} (Theoretical value) [N]	F_{t_max} (3D FEM value) [N]
37.2	38.8

$B_{\max}$ increased with l_a because of the decreased cross-section of the armature core, as shown in Fig. 7(d).

The optimal design point was approximately equal to, but below, $l_a = 2.625$ mm, as shown in Fig. 7(d). Above $l_a = 2.625$ mm, where the theoretical value of $B_{\max}$ was over 1.5 T, there are differences between theoretical and 3-D FEM values because the iron core starts to saturate. Therefore, we decided to use the optimal design point as $l_a = 2.5$ mm, considering the thickness of the iron core, which was 0.5 mm [8].

The theoretical value of $F_{t\_\max}$ at this point was 37.2 N, almost the same as the 3-D FEM value as shown in Table III. The armature core width l_z was 4 mm, and the number of winding turns per armature pole was 73 turns.

V. CONCLUSION

In this paper, a double-sided transverse flux PMLSM to address the problem of complex structure with TFMs was proposed. The advantages of the proposed configuration are its simplified structure, the use of lamination, and the small sensitivity of normal attractive force to assembly error achieved through consideration of the magnetic circuit. These advantages are helpful for easy TFM manufacture.

In addition, a design method for the maximum thrust in nonsaturation region was proposed as a simple design method in the preliminary design stage. In the process of the optimal design for maximum thrust in nonsaturation region, it is important to confirm whether certain design point is in saturation region or not. This is determined by the maximum flux at certain design point and it is affected by electric and magnetic loads at that point. In the proposed method, the maximum flux and its position, the optimal point, and thrust at the point is simply estimated from flux calculations at only $z = 0$ and 0.5 τ_p, using a

2-D ERN method. Also, there is a good agreement between theoretical and 3-D FEM values. Therefore, the proposed method is useful as a simple design method for maximum thrust in the preliminary stage.

Future studies will involve further analysis of the prototype model through experimental verification, including thrust, thrust ripple, and positioning accuracy.

REFERENCES

[1] H. Weh, "Permanenterregte Synchronmaschine hoher Kraftdichte nach dem Transversalflusskonzept," *etzArchiv*, vol. 10, pp. 143–149, 1988.

[2] S. D. Joao and V. Mauricio, "Transverse flux machine: What for?," *IEEE Multidisciplinary Eng. Edu. Ma.*, vol. 2, no. 1, pp. 4–6, 2007.

[3] M. Zhao, Q. Wang, J. Zou, and G. Wu, "Development and analysis of tubular transverse flux machine with permanent-magnet excitation," *IEEE Trans. Ind. Electron.*, vol. 59, no. 5, pp. 2198–2207, May 2012.

[4] J. S. Shin, T. Koseki, and H. J. Kim, "Proposal and design of short armature core double-sided transverse flux type linear synchronous motor," *IEEE Trans. Magn.*, vol. 48, no. 11, pp. 3871–3874, Nov. 2012.

[5] M. Siatkowski and B. Orlik, "Influence of saturation effects in a transverse flux machine," in *Proc. 13th Power Electron. Motion Contr. Conf. (EPE-PEMC)*, 2008, pp. 830–836.

[6] H. Polinder, J. G. Slootweg, M. J. Hoeijmakers, and J. C. Compter, "Modeling of a linear PM machine including magnetic saturation and end effects: Maximum force-to-current ratio," *IEEE Trans. Magn.*, vol. 39, no. 6, pp. 1681–1688, Jun. 2003.

[7] Y. Misawa, S. Sugita, and S. Onodera, "Linear servo motor: Double-sided core type model," *SANYO DENKI Tech. Rep.*, no. 15, pp. 25–27, 2003, written in Japanese.

[8] JFE Steel Corp. [Online]. Available: http://www.jfe-steel.co.jp/

[9] Shin-Etsu Chemical Co., Ltd. [Online]. Available: http://www.shinetsu.co.jp/j/index.shtml

[10] B. Sheikh-Ghalavand, S. Vaez-Zadeh, and A. H. Isfahani, "An improved magnetic equivalent circuit model for iron-core linear permanent-magnet synchronous motors," *IEEE Trans. Magn.*, vol. 46, no. 1, pp. 112–120, Jan. 2010.

[11] JSOL Corp. [Online]. Available: http://www.jmag-international.com/

[12] T. Nakamura, T. Koseki, and Y. Aoyama, "A low-speed high-torque permanent magnet synchronous motor—Reducing cogging torque and eddy current loss—," *Jap. Soc. Appl. Electromagnet. Mechan.*, vol. 20, no. 2, pp. 410–415, 2012.